International Journal of Heat and Mass Transfer 52 (2009) 4938–4945

Contents lists available at ScienceDirect

International Journal of Heat and Mass Transfer

journal homepage: www.elsevier.com/locate/ijhmt

Theoretical analysis of premixed low-velocity filtration combustion for Lewis number different from one

A. Knyazeva [a], V. Bubnovich [b,*], C. Rosas [c], N. Moraga [c]

[a] Institute of Strength Physics and Material Science, Tomsk, Russia
[b] Department of Chemical Engineering, Universidad de Santiago de Chile, Casilla 10233, Santiago, Chile
[c] Department of Mechanical Engineering, Universidad de Santiago de Chile, Casilla 10233, Santiago, Chile

ARTICLE INFO

Article history:
Received 17 June 2008
Received in revised form 16 April 2009
Accepted 16 April 2009
Available online 4 July 2009

Keywords:
Lean mixture
Low-velocity filtration combustion
Analytical solution

ABSTRACT

An exact analytical solution for the stationary reaction front propagation in an inert porous media is obtained in the approximation of the narrow reaction zone. It is assumed that the similarity of the temperature and concentration fields does not take a place. The applicability of the solution found for gas and solid disequilibrium temperature distributions in the reactants region and behind the reaction front approximate evaluations is illustrated with the help of one special example.

1. Introduction

Recently, the combustion of gases in porous media has been the focus of numerous researchers working in the field of combustion and the environment due to its interesting industrial applications [1–4] such as oil extraction, infrared burners and heater development, ceramic materials synthesis, porous catalysts, grounds polluted by toxic organic shedding recovery, destruction of volatile organic compounds (VOC) in air, hydrogen production, diesel engines, and pollution control.

The process by which the region of exothermic chemical reactions propagates along inert porous media must be viewed within the framework of combustion waves in these types of media, as shown schematically in Fig. 1. It is known from the literature [5–7] that during gas mixture combustion in inert porous media, combustion waves that move upstream or downstream along the system can be seen. The direction of these movements depends generally on the physical properties of both solid and gas as well as on initial speed, temperature, and excess air of the mixture. Conjugating these parameters, wave speeds achieved are much lower than those of the gas, and the temperature profiles show a very pronounced maximum in the reaction region.

Due to the active participation in this process of both the porous medium and the reacting gas, three characteristic regions can be identified inside the porous medium. There is a region in front of the combustion region where reacting gases are mixed in naturally and preheated using heat lost by the porous medium. At the entrance of this region, the temperature, the gas speed, and the equivalence ratio are controlled. In the same region of the porous medium, $0 < z < l_1$, the gaseous mixture is ignited as a result of preheating of a porous medium zone several centimeters in length by an external heat source (an electric resistance, for example).

The second region is a luminous tight one, and it represents the chemical reaction region which moves in the same direction or against the gas flow, and it is here where a huge amount of enthalpy is absorbed by the porous medium and directed to the first region where the fresh mixture enters. Because of the large specific surface of the porous medium, this last region delivers energy to the incoming gas mixture which is transferred by convection to the reaction region. Thus, heat regeneration occurs which implies an enthalpy excess at the chemical reaction region and a partial increase of the front temperature, which can exceed the adiabatic temperature [8,9]. Moreover, mass transport by diffusion and heat transport by thermal radiation are considerable at this region.

Finally, there is a third region which is located forward of the front and has combustion products, which actively exchanges heat by convection with the porous medium, leaving the system at almost ambient temperature. These systems are characterized by the presence of two dynamic fronts: the chemical reaction front and the high-temperature front. As a result of the adequate selection of geometric properties, dynamic flows, and thermal parameters, the two fronts can superimpose and intensify reciprocally.

Today, gas combustion in inert porous media is intensively studied. There are numerical [10,11], analytical [12,13], and

* Corresponding author. Tel.: +56 2 7181805.
E-mail addresses: anna@ms.tsc.ru (A. Knyazeva), vbubnovi@lauca.usach.cl (V. Bubnovich).

0017-9310/$ - see front matter © 2009 Published by Elsevier Ltd.
doi:10.1016/j.ijheatmasstransfer.2009.04.015

Nomenclature

c	specific heat (J/kg K)
D	mass diffusion coefficient (m^2/s)
E_a	activation energy (J/mol)
k	frequency factor (1/s)
Le	Lewis number
Q	enthalpy of combustion (J/kg)
T	temperature (K)
T_m	maximum temperature in the reaction front (K)
T_0	environment temperature (K)
t	time (s)
u	gas velocity (m/s)
V_n	normal component of the combustion front velocity (m/s)

Greek symbols

α	heat exchange coefficient (W/m^3 K)
β	heat loss to the environment (W/m^3 K)
λ	thermal conductivity (W/m K)
ε	porosity
η	fuel mass fraction
ρ	density (kg/m^3)

Subscripts

0	initial condition
g	gas
s	solid

Superscripts

0	stationary conditions

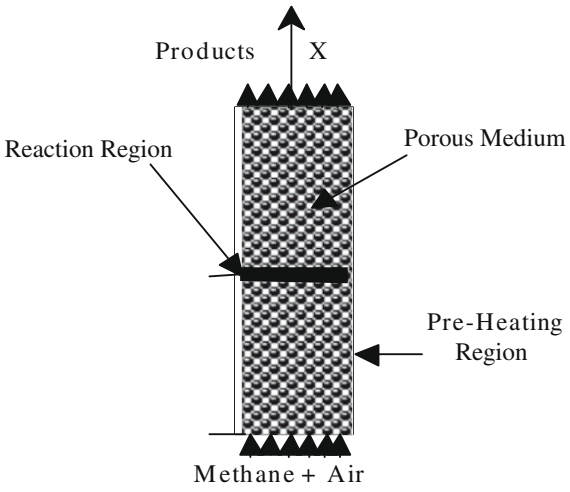

Fig. 1. Scheme of the physical problem considered.

experimental studies [9,14,15] of the topic, where relations are established as formulas or graphics between major properties of a combustion wave such as the highest temperature, the speed, and the wave direction of motion and the two-phase system physical properties and conditions at the inlet. In spite of this, there are relatively few studies of the mixture ignition temperature in the two-phase system and the thickness of the chemical reaction region. Normally, to ignite a mixture in the numerical studies [16], a temperature not lower than that required is imposed on a region of several centimeters of extension in the inert porous medium.

However, in practice it is very important to know the precise value of this temperature, because higher temperatures compromise solid materials and originate toxic gases. In analytical solutions, the combustion region thickness is normally ignored in order to be able to integrate the energy equation, in which the right side has an extremely non-linear term.

Akkutlu and Yortsos [17] studied the properties of forward combustion fronts propagating at a constant velocity in the presence of heat losses. Heat losses are assumed to be relatively small and are expressed using two models: (1) a convective type, using an overall heat transfer coefficient; and (2) a conductive type, for heat transfer by transverse conduction to infinitely large surrounding formations. As the main results they develop expressions for temperature and concentration profiles and the velocity of the combustion front, under both adiabatic and non-adiabatic conditions, in analytical form. An explicit expression is also obtained for the effective heat transfer coefficient in terms of the reservoir thickness and the front propagation speed. This coefficient is not only dependent on the thermal properties of the porous medium but also on the front dynamics.

Kennedy et al. [18] described the chemical structures of methane–air filtration combustion waves in a range of equivalence ratios from 0.2 to 2.5. Downstream, upstream, and standing waves were observed in the experiments. For equivalence ratios in the range of 0.45–1.7 at an inlet velocity of 0.25 m/s, downstream wave propagation occurred, corresponding to the super adiabatic combustion. With further increase (>1.7) or decrease (<0.45) of the equivalence ratio, the propagation regime changed to upstream and the maximum temperature in the packed bed was no longer higher than the adiabatic temperature for the specific inlet mixtures. The accompanying numerical simulation considered a fully developed steady combustion wave using a one-temperature model.

Shkadinsky et al. [19] showed the existence of both one and two stationary reaction zone structures which arise in filtration combustion in a moving porous medium. Using the narrow reaction zone approximation, they derive approximate analytical expressions for the principal combustion characteristics, including combustion temperature, the temperature and depth of solid conversion at the first reaction zone, the locations of the reaction zones, the inlet and outlet oxidant fluxes, as well as profiles for the spatial distributions of pressure, temperature, and depth of conversion, corresponding to the stationary reaction zone structures.

Foutko et al. [12] present an analytical solution of this combustion wave assuming that the reaction speed in the combustion region is infinite and that the longitudinal extension of said region is null. Nevertheless, the construction of an analytical solution is here achieved without the help of those last two assumptions. It is known [20,21] that the greater the extension of the combustion region, the higher the production of NO_x at the front, and consequently it would be interesting to find out about the dependence of the thickness of that region on the rest of the physical parameters involved in the studied problem.

The conditions for the propagation of the steady combustion front in terms of the governing parameters for filtration combustion of a solid fuel in a reservoir that consist of two layers of different permeability and thickness have been investigated by

Akkutlu and Yortsos [22]. They found that heterogeneity reduces the front temperature in the high-permeability layer and uncouples the propagation of the combustion front in the two layers.

Recently, Bubnovich et al. [23] presented analytical solutions for the temperature and mass fractions of methane/air mixture combustion in a packed bed. The solutions were built in three different regions: the preheating region, the reaction region, and the combustion products region. Based on the solutions, the extension of the reaction region, the ignition temperature, and the combustion wave speed were also predicted. In their analysis a one-temperature model was used and the methane oxidation mechanism was reduced to a global chemical reaction in a single step. However, it is important to consider the situations in which the interfacial heat transfer coefficient has a specific value and affects the characteristics of the combustion wave. Therefore, a study was made of self-sustaining combustion waves by Bubnovich and Toledo [24] during the filtration of lean methane–air mixtures in inert porous media using the two-temperature approximation that considers the characteristics of the reaction region.

Jun-Rui Shi et al. [25] investigated combustion wave characteristics of lean pre-mixtures in a porous medium burner. Based on the flame sheet assumption, a relationship between the combustion wave speed and the maximum combustion temperature was given. Then an approach from the laminar premixed flame theory is applied and the entire flame zone is divided into a preheating region and a reaction region, and treated separately. In this way the second relationship between the two parameters is deduced. Thus, a closed analytical solution for the combustion wave speed and the maximum combustion temperature is obtained. Over a wide range of working conditions, the numerical predictions and theoretical results show qualitative agreement with experimental data available from the literature. The results reveal that the mechanism of super adiabatic combustion is attributed to the overlapping of the thermal wave and combustion wave under certain conditions.

The study of combustion, including combustion in porous media, usually considers that mass diffusion and heat conduction are similar [26] in cases in which the Lewis number *Le* is equal to one. However, in a real situation, depending on the gas mixture composition, *Le* can deviate from unity, and that can lead to some interesting phenomena [27]. There are analytical approximations in simple combustion models for gases that take into account the difference between thermal conduction and mass diffusion coefficients [28]. Because analytical solution for combustion in porous media are not found in the open literature, this paper present an original exact analytical solution to the stationary combustion wave propagation in a porous medium, based on the narrow reaction approximation.

2. Problem formulation

The mathematical model of gas combustion in a porous medium for the physical situation presented in Fig. 1 is based on a two-temperature formulation [12,24]. The assumptions used include that the chemical reaction can be described by a one-step reaction scheme (reactants–product), the reaction front is plane, and the gas mixture properties do not depend on the temperature. Porous media filled in the packed bed are non-catalytic, homogeneous, and optically thick. The working gas is non-radiating, the gas flow in the porous medium is laminar, and pressure loss in the burner is neglected. In this case the mathematical formulation of the problem includes the energy equations for the gas and the solid phases, as well as the conservation equation for the chemical species, respectively:

$$\rho_g c_g\left(\frac{\partial T_g}{\partial t}+u\frac{\partial T_g}{\partial x}\right)=\frac{\partial}{\partial x}\left(\lambda_g\frac{\partial T_g}{\partial x}\right)-\frac{a}{\varepsilon}(T_g-T_s)+Qk\eta exp\left(-\frac{E_a}{RT_g}\right), \quad (1)$$

$$\frac{\partial \eta}{\partial t}+u\frac{\partial \eta}{\partial x}=\frac{\partial}{\partial x}\left(D\frac{\partial \eta}{\partial x}\right)-k\eta exp\left(-\frac{E_a}{RT_g}\right), \quad (2)$$

$$\rho_s c_s\frac{\partial T_s}{\partial t}=\frac{\partial}{\partial x}\left(\lambda_s\frac{\partial T_s}{\partial x}\right)+\frac{a}{1-\varepsilon}(T_g-T_s)-\frac{\beta}{1-\varepsilon}(T_s-T_0), \quad (3)$$

where T is the temperature, η is the fuel mass fraction; x is the space coordinate in the direction of the front propagation; a is the heat exchange coefficient between the gas and solid phases; u is the gas velocity, ρ, c, λ are density, heat capacity, and thermal conductivity; D is the mass diffusion coefficient; ε is the porosity; and k, E_a, Q are the frequency factor, activation energy, and enthalpy of combustion, respectively; the coefficient β describes the heat loss to the environment by thermal radiation and natural convection, T_0 is the ambient temperature, and the subscripts s and g are related, to the solid and gas phase, respectively.

Assuming, that the reaction front is narrow, a conjugate formulation with boundary condition between the reactants and products can be built. Supposing, that the reaction front moves at speed V_n, the mathematical formulation (1)–(3) becomes the following:

$$\rho_g c_g\left(\frac{\partial T_g}{\partial t}+(u+V_n)\frac{\partial T_g}{\partial x}\right)=\frac{\partial}{\partial x}\left(\lambda_g\frac{\partial T_g}{\partial x}\right)-\frac{a}{\varepsilon}(T_g-T_s), \quad (4)$$

$$\frac{\partial \eta}{\partial t}+(u+V_n)\frac{\partial \eta}{\partial x}=\frac{\partial}{\partial x}\left(D\frac{\partial \eta}{\partial x}\right), \quad (5)$$

$$\rho_s c_s\left(\frac{\partial T_s}{\partial t}+V_n\frac{\partial T_s}{\partial x}\right)=\frac{\partial}{\partial x}\left(\lambda_s\frac{\partial T_s}{\partial x}\right)+\frac{a}{1-\varepsilon}(T_g-T_s)-\frac{\beta}{1-\varepsilon}(T_s-T_0), \quad (6)$$

These equations are valid before ($x < 0$) and after the reaction front ($x > 0$), where V_n is the normal component of the combustion front velocity.

In the reaction front, at $x = 0$, between the reactants and products, the following boundary conditions are valid:

$$\left.\frac{\partial T_g}{\partial x}\right|_{-0}-\left.\frac{\partial T_g}{\partial x}\right|_{+0}=Q\frac{V_n}{\lambda_g},\quad T_g|_{-0}=T_g|_{+0}, \quad (7)$$

$$\lambda_s\left.\frac{\partial T_s}{\partial x}\right|_{-0}-\lambda_s\left.\frac{\partial T_s}{\partial x}\right|_{+0}=0,\quad T_s|_{-0}=T_s|_{+0}, \quad (8)$$

$$D\left.\frac{\partial \eta}{\partial x}\right|_{-0}-D\left.\frac{\partial \eta}{\partial x}\right|_{+0}=V_n,\quad \eta|_{-0}=\eta|_{+0}. \quad (9)$$

The following initial and boundary conditions are imposed:

$$t=0,\ x=0:\ T_g=T_0,\quad T_s=T_0,\quad \eta=1. \quad (10)$$

$$x\to\infty:\ \frac{\partial T_g}{\partial x}=0,\quad \frac{\partial T_s}{\partial x}=0,\quad \frac{\partial \eta}{\partial x}=0. \quad (11)$$

The mathematical model can be formulated in terms of dimensionless variables using the following scales,

$$\theta_s=\frac{T_s-T_0}{T_m-T_0},\quad \theta_g=\frac{T_g-T_0}{T_m-T_0},\quad \xi=\frac{V_n}{\kappa}x,\quad \tau=\frac{V_n^2}{\kappa}t, \quad (12)$$

where T_m is the maximum temperature in the reaction front, which is found later, and $\kappa=\frac{\lambda_g}{c_g\rho_g}$ is the thermal diffusivity. Then, the nondimensional mathematical model takes the form

$$\frac{\partial \theta_g}{\partial \tau}+(1+\bar{u})\frac{\partial \theta_g}{\partial \xi}=\frac{\partial^2\theta_g}{\partial \xi^2}-\frac{A}{\varepsilon}(\theta_g-\theta_s); \quad (13)$$

$$\frac{\partial \eta}{\partial \tau}+(1+\bar{u})\frac{\partial \eta}{\partial \xi}=Le\frac{\partial^2\eta}{\partial \xi^2}; \quad (14)$$

$$K_c\left[\frac{\partial \theta_s}{\partial \tau}+\frac{\partial \theta_s}{\partial \xi}\right]=K_\lambda\frac{\partial^2\theta_s}{\partial \xi^2}+\frac{A}{1-\varepsilon}(\theta_g-\theta_s)-\frac{BK_c}{1-\varepsilon}\theta_s. \quad (15)$$

The boundary conditions are:

$$\xi = 0:$$

$$\left.\frac{\partial\theta_g}{\partial\xi}\right|_{-0} - \left.\frac{\partial\theta_g}{\partial\xi}\right|_{+0} = \Delta\frac{V_n}{V_n^0}, \quad \theta_g|_{-0} = \theta_g|_{+0} = 1; \tag{16}$$

$$\left.\frac{\partial\theta_s}{\partial\xi}\right|_{-0} - \left.\frac{\partial\theta_s}{\partial\xi}\right|_{+0} = 0, \quad \theta_s|_{-0} = \theta_s|_{+0}; \tag{17}$$

$$\left.\frac{\partial\eta}{\partial\xi}\right|_{-0} - \left.\frac{\partial\eta}{\partial\xi}\right|_{+0} = \frac{V_n}{V_n^0}\frac{1}{Le}, \quad \eta|_{-0} = \eta|_{+0}; \tag{18}$$

$$\xi \to -\infty: \ \theta_g = 0, \quad \theta_s = 0, \quad \eta = 1; \tag{19}$$

$$\xi \to +\infty: \ \frac{\partial\theta_g}{\partial\xi} = 0, \quad \frac{\partial\theta_s}{\partial\xi} = 0, \quad \frac{\partial\eta}{\partial\xi} = 0, \tag{20}$$

where

$$\bar{u} = \frac{u}{V_n}; \quad A = \frac{at_*}{c_g\rho_g}; \quad Le = \frac{Dc_g\rho_g}{\lambda_g}; \quad B = \frac{\beta t_*}{c_s\rho_s};$$
$$K_c = \frac{c_s\rho_s}{c_g\rho_g}; \quad K_\lambda = \frac{\lambda_s}{\lambda_g}; \quad \Delta = \frac{Q}{c_g\rho_g(T_m - T_0)} \tag{21}$$

are the dimensionless problem parameters.

In a general case it is necessary to find the stationary solutions and to investigate their stability to small perturbations. In this paper we restrict the investigation to the stationary problem.

3. Stationary problem solution

The stationary problem is obtained when the time derivatives set are equal to zero in Eqs. (13)–(15). Assuming that the stationary front velocity $V_n = V_n^0$, the stationary problem in the mathematical model, for $\xi < 0$ and $\xi > 0$, is defined by the following equations:

$$(1+\bar{u})\frac{d\theta_g}{d\xi} = \frac{d^2\theta_g}{d\xi^2} - \frac{A}{\varepsilon}(\theta_g - \theta_s); \tag{22}$$

$$(1+\bar{u})\frac{d\eta}{d\xi} = Le\frac{d^2\eta}{d\xi^2}; \tag{23}$$

$$K_c\frac{d\theta_s}{d\xi} = K_\lambda\frac{d^2\theta_s}{d\xi^2} + \frac{A}{1-\varepsilon}(\theta_g - \theta_s) - \frac{BK_c}{1-\varepsilon}\theta_s \tag{24}$$

and the boundary conditions in the interface between the reactants and the products (for $\xi = 0$) are

$$\left.\frac{d\theta_g}{d\xi}\right|_{-0} - \left.\frac{d\theta_g}{d\xi}\right|_{+0} = \Delta, \quad \theta_g|_{-0} = \theta_g|_{+0} = 1; \tag{25}$$

$$\left.\frac{d\theta_s}{d\xi}\right|_{-0} - \left.\frac{d\theta_s}{d\xi}\right|_{+0} = 0, \quad \theta_s|_{-0} = \theta_s|_{+0}; \tag{26}$$

$$\left.\frac{d\eta}{d\xi}\right|_{-0} - \left.\frac{d\eta}{d\xi}\right|_{+0} = \frac{1}{Le}, \quad \eta|_{-0} = \eta|_{+0}; \tag{27}$$

$$\xi \to -\infty: \ \theta_g = 0, \quad \theta_s = 0, \quad \eta = 1; \tag{28}$$

$$\xi \to +\infty: \ \frac{d\theta_g}{d\xi} = 0, \quad \frac{d\theta_s}{d\xi} = 0, \quad \frac{d\eta}{d\xi} = 0. \tag{29}$$

A system of the three linear, second order, ordinary differential equations (22)–(24) is obtained. A more convenient form for the mathematical model can be found introducing the new additional notation

$$y = \frac{d\theta_g}{d\xi}; \quad z = \frac{d\eta}{d\xi}; \quad v = \frac{d\theta_s}{d\xi}. \tag{30}$$

As a result, a conjugate model is obtained that includes a system of the six ordinary first order differential equations (31)–(36):

$$\frac{d\theta_g}{d\xi} = y; \tag{31}$$

$$\frac{dy}{d\xi} = (1+\bar{u})y + \frac{A}{\varepsilon}(\theta_g - \theta_s); \tag{32}$$

$$\frac{d\eta}{d\xi} = z; \tag{33}$$

$$Le\frac{dz}{d\xi} = (1+\bar{u})z; \tag{34}$$

$$\frac{d\theta_s}{d\xi} = v; \tag{35}$$

$$K_\lambda\frac{dv}{d\xi} = K_c v - \frac{A}{1-\varepsilon}(\theta_g - \theta_s) + \frac{B}{1-\varepsilon}K_c\theta_s, \tag{36}$$

which can be presented in a vectorial notation:

$$\vec{Y}' = \mathbf{A}\vec{Y}, \tag{37}$$

where the unknown vector and the coefficient matrix are:

$$\vec{Y} = (\theta_g, y, \eta, z, \theta_s, v) \tag{38}$$

and

$$\mathbf{A} = \begin{bmatrix} 0 & 1 & 0 & 0 & 0 & 0 \\ \frac{A}{\varepsilon} & 1+\bar{u} & 0 & 0 & -\frac{A}{\varepsilon} & 0 \\ 0 & 0 & 0 & 1 & 0 & 0 \\ 0 & 0 & 0 & \frac{1+\bar{u}}{Le} & 0 & 0 \\ 0 & 0 & 0 & 0 & 0 & 1 \\ \gamma & 0 & 0 & 0 & \alpha & \frac{K_c}{K_\lambda} \end{bmatrix}, \tag{39}$$

respectively, with the following symbols:

$$\gamma = -\frac{A}{(1-\varepsilon)K_\lambda}, \quad \alpha = \frac{BK_c}{(1-\varepsilon)K_\lambda} + \frac{A}{(1-\varepsilon)K_\lambda} = \frac{BK_c}{(1-\varepsilon)K_\lambda} + \gamma. \tag{40}$$

Eqs. (33) and (34) are independent from the rest of the system and can be solved separately. Therefore, the resulting four residual equations (31), (32), (35) and (36) of the system have the following expression for the coefficients matrix:

$$\mathbf{A} = \begin{bmatrix} 0 & 1 & 0 & 0 \\ \frac{A}{\varepsilon} & 1+\bar{u} & -\frac{A}{\varepsilon} & 0 \\ 0 & 0 & 0 & 1 \\ \gamma & 0 & \alpha & \frac{K_c}{K_\lambda} \end{bmatrix}. \tag{41}$$

The characteristic equation, defined by

$$\mathbf{A} - \lambda\mathbf{E} = 0 \tag{42}$$

allows finding the existence condition of the non-trivial solution for the differential equations system. Calculating the determinant, the result obtained is

$$\frac{A^2}{\varepsilon(1-\varepsilon)K_\lambda} + \left[\lambda(1+\bar{u}) - \lambda^2 + \frac{A}{\varepsilon}\right]\left(\lambda\frac{K_c}{K_\lambda} + \alpha - \lambda^2\right) = 0. \tag{43}$$

The characteristic equation (43) has, naturally, four roots, which are the eigenvalues of the matrix (41). The full matrix (39) has two additional eigenvalues that can be calculated in an exact way:

$$\lambda = 0; \quad \lambda = \frac{1+\bar{u}}{Le}. \tag{44}$$

In the particular case, when $A = 0$, the heat exchange between the solid and gas phases is absent, and hence Eq. (43) is reduced to

$$[\lambda(1+\bar{u}) - \lambda^2]\left(\lambda\frac{K_c}{K_\lambda} + \frac{\widehat{A}K_c}{(1-\varepsilon)K_\lambda} - \lambda^2\right) = 0. \tag{45}$$

Each pair of roots of this equation corresponds to the two independent stationary thermal conductivity problems in the gas ($\lambda_1 = 0, \lambda_2 = 1 + \bar{u}$) and the solid $\left(\lambda_{3,4} = \frac{K_c}{K_\lambda}\left[1 \pm \sqrt{1 + \frac{4B}{(1-\varepsilon)}\frac{K_\lambda}{K_c}}\right]\right)$ phase. In this case, the solution has the form

$$\theta_g^- = \frac{\Delta}{1+\bar{u}} exp((1+\bar{u})\xi); \quad \theta_g^+ = \frac{\Delta}{1+\bar{u}}; \tag{46}$$

$$\eta^- = 1 - \frac{1}{1+\bar{u}} exp\left(\frac{1+\bar{u}}{Le}\xi\right); \quad \eta^+ = \frac{\bar{u}}{1+\bar{u}}; \tag{47}$$

$$\theta_s = 0. \tag{48}$$

Assuming that $\frac{\Delta}{1+\bar{u}} = 1$, the maximum temperature in the front can be found.

In the general case, when $A \neq 0$, the four previous equations cannot be separated. If all roots of the characteristic equation are real values, the eigenvector $\mathbf{a}_i$ of matrix $\mathbf{A}$ with components a_{ij} corresponds to each eigenvalue λ_i. Then the columns $\mathbf{a}_i \boldsymbol{exp}(\lambda_i\xi)$ form the fundamental solution system. In this case, the general solution of the ordinary differential equation system can be written in the form

$$y_i = C_1 a_{1i} exp(\lambda_1\xi) + C_2 a_{2i} exp(\lambda_2\xi) + C_3 a_{3i} exp(\lambda_3\xi) + C_4 a_{4i} exp(\lambda_4\xi), \quad i = 1,2,3,4. \tag{49}$$

Eq. (49) contains four arbitrary constant C_i and represents a solution for a chemical species y_i. To find the eigenvectors, it is necessary to solve the four-equation system for each eigenvalue λ_i:

$$(\mathbf{A} - \lambda_i \mathbf{E})\mathbf{a}_i = 0. \tag{50}$$

In order to solve the problem, the cofactor A_{ij} in the first column of the matrix $(\mathbf{A} - \lambda_i\mathbf{E})$ can be used as the eigenvalue component $\mathbf{a}_i$:

$$A_{ij} = (-1)^{i+j} M_{ij}, \tag{51}$$

where the minor M_{ij} is the determinant of the sub matrix obtained by deleting row i, column j of the matrix.

The analysis shows that in this case the cofactors in the second column of the matrix are the most desirable. Therefore,

$$\begin{aligned} a_{i1} &= -\lambda_i^2 + \frac{K_c}{K_\lambda}\lambda_i + \alpha; \\ a_{i2} &= -\lambda_i^3 + \frac{K_c}{K_\lambda}\lambda_i^2 + \alpha\lambda_i \\ a_{i3} &= -\gamma; \\ a_{i4} &= -\gamma\lambda_i. \end{aligned} \tag{52}$$

Even and odd values of the coefficients are related by the next equation:

$$a_{i2} = \lambda_i a_{i1}; \quad a_{i4} = \lambda_i a_{i3}. \tag{53}$$

The analysis shows that the characteristic equation can have complex roots with positive and negative real parts; and it can also have multiple roots, in which case, if they exist, the problem needs to be viewed in a special way. Obviously, in the region of variation of the physical parameters of the mathematical model all the roots are real: two of them are negative (λ_1, $\lambda_2 < 0$) and two are positive (λ_3, $\lambda_4 > 0$).

Then, considering the conditions in the reactants and in the products, a general solution of the following form is obtained:

$$\begin{aligned} \theta_g^- &= C_3^- a_{31} exp(\lambda_3\xi) + C_4^- a_{41} exp(\lambda_4\xi); \\ \theta_s^- &= C_3^- a_{33} exp(\lambda_3\xi) + C_4^- a_{43} exp(\lambda_4\xi); \\ \theta_g^+ &= C_1^+ a_{11} exp(\lambda_1\xi) + C_2^+ a_{21} exp(\lambda_2\xi); \\ \theta_s^+ &= C_1^+ a_{13} exp(\lambda_1\xi) + C_2^+ a_{23} exp(\lambda_2\xi). \end{aligned} \tag{54}$$

Using the boundary conditions in the front (25)–(29), the system of equations to determine the integration constants is

$$\begin{aligned} &C_3^- a_{31} + C_4^- a_{41} = C_1^+ a_{11} + C_2^+ a_{21} = 1; \\ &C_3^- a_{33} + C_4^- a_{43} = C_1^+ a_{13} + C_2^+ a_{23}; \\ &C_3^- a_{31}\lambda_3 + C_4^- a_{41}\lambda_4 = C_1^+ a_{11}\lambda_1 + C_2^+ a_{21}\lambda_2 + \Delta; \\ &C_3^- a_{33}\lambda_3 + C_4^- a_{43}\lambda_4 = C_1^+ a_{13}\lambda_1 + C_2^+ a_{23}\lambda_2, \end{aligned} \tag{55}$$

where the temperature in the front is equal to one in accordance with the choice of the dimensionless variable. Since there are four integration constants and five boundary conditions in the interface between the reactants and the products, the expression for parameter Δ can be found, and hence the maximum temperature in the reaction front, T_m, can be determined.

With the help of Eqs. (52) and (53), system (55) may be presented in the following form:

$$\begin{aligned} &C_3^- a_3 + C_4^- a_4 = C_1^+ a_1 + C_2^+ a_2 = 1; \\ &C_3^- + C_4^- = C_1^+ + C_2^+; \\ &C_3^- a_3\lambda_3 + C_4^- a_4\lambda_4 = C_1^+ a_1\lambda_1 + C_2^+ a_2\lambda_2 + \Delta; \\ &C_3^-\lambda_3 + C_4^-\lambda_4 = C_1^+\lambda_1 + C_2^+\lambda_2, \end{aligned} \tag{56}$$

where

$$a_i = -\lambda_i^2 + \frac{K_c}{K_\lambda}\lambda_i + \alpha. \tag{57}$$

This equation system can be solved in an explicit form, to obtain

$$\begin{aligned} C_1^+ &= -\frac{a_2(a_3-a_4)(\Delta+\lambda_2-\lambda_3) + a_4(a_2-a_3)(\lambda_4-\lambda_3)}{a_4a_3(a_1-a_2)(\lambda_4-\lambda_3) - a_1a_2(a_3-a_4)(\lambda_2-\lambda_1)}; \\ C_2^+ &= \frac{a_1(a_3-a_4)(\Delta+\lambda_1-\lambda_3) + a_4(a_1-a_3)(\lambda_4-\lambda_3)}{a_4a_3(a_1-a_2)(\lambda_4-\lambda_3) - a_1a_2(a_3-a_4)(\lambda_2-\lambda_1)}; \\ C_3^- &= -\frac{a_4(a_1-a_2)(\Delta+\lambda_1-\lambda_4) + a_2(a_1-a_4)(\lambda_2-\lambda_1)}{a_3a_4(a_1-a_2)(\lambda_4-\lambda_3) - a_1a_2(a_3-a_4)(\lambda_2-\lambda_1)}; \\ C_4^- &= \frac{a_3(a_1-a_2)(\Delta+\lambda_1-\lambda_3) + a_2(a_1-a_3)(\lambda_2-\lambda_1)}{a_3a_4(a_1-a_2)(\lambda_4-\lambda_3) - a_1a_2(a_3-a_4)(\lambda_2-\lambda_1)}; \\ \Delta &= \frac{\lambda_1\lambda_2(a_3-a_4)(a_1-a_2) + (a_2-a_4)(a_3-a_1)(\lambda_3\lambda_1+\lambda_2\lambda_4) + (a_2-a_3)(a_1-a_4)(\lambda_1\lambda_4+\lambda_2\lambda_3)}{(a_1-a_2)(\lambda_4a_3-a_4\lambda_3) + (a_3-a_4)(\lambda_1a_2-a_1\lambda_2)}. \end{aligned} \tag{58}$$

The solution for the reactant concentration in this stationary problem takes the form of Eq. (47), as it is the simplest case when $A = 0$.

Assuming $K_c \approx 1$, $K_\lambda \approx 100$, $\bar{u} \approx -10^3$, that is originated when $|U_g/V_n| >> 1$, $c_g\rho_g \approx c_s\rho_s$, $\lambda_g << \lambda_s$, an interesting limit case is obtained, in which the solution can be presented in the form

$$\begin{aligned}\theta_g^- &= C_3^- a_{31} + C_4^- a_{41} exp(\lambda_4 \xi);\\ \theta_s^- &= C_3^- a_{33} + C_4^- a_{43} exp(\lambda_4 \xi);\\ \theta_g^+ &= C_2^+ a_{21} exp(\lambda_2 \xi);\\ \theta_s^+ &= C_2^+ a_{23} exp(\lambda_2 \xi).\end{aligned} \tag{59}$$

The analysis of the characteristic equation gives

$$|\lambda_1| >> |\lambda_2|, \quad |\lambda_4| >> |\lambda_3|.$$

Since the equalities in Eq. (59) hold near the vicinity of the reaction front, the additional condition is assumed to apply to the reactants:

$$C_3^- = 0. \tag{60}$$

This can be verified by Eq. (59). Considering the estimates of the physical parameters above, the result obtained is:

$$\frac{A^2}{\varepsilon(1-\varepsilon)K_\lambda} << 1 \quad \text{or} \quad \frac{\alpha^2\kappa^3}{\varepsilon(1-\varepsilon)V_n^4\lambda_s} << 1. \tag{61}$$

The following approximate characteristic equation roots values can be used

$$\begin{aligned}&\lambda_1 \approx 1+\bar{u} \approx \bar{u} < 0; \quad \lambda_2 \approx \frac{1}{2}\frac{K_c}{K_\lambda}\left[1-\sqrt{1+4\alpha\left(\frac{K_\lambda}{K_c}\right)^2}\right] < 0;\\ &\lambda_3 \approx -\frac{A}{\varepsilon(1+\bar{u})} > 0; \quad \lambda_4 \approx \frac{1}{2}\frac{K_c}{K_\lambda}\left[1+\sqrt{1+4\alpha\left(\frac{K_\lambda}{K_c}\right)^2}\right] > 0.\end{aligned} \tag{62}$$

In the case when $\bar{u} \approx 10^3 > 0$, we have that

$$|\lambda_2| << |\lambda_1|, \quad |\lambda_3| >> |\lambda_4|,$$

and a general solution of the following type is obtained

$$\begin{aligned}\theta_g^- &= C_3^- a_{31} exp(\lambda_3 \xi);\\ \theta_s^- &= C_3^- a_{33} exp(\lambda_3 \xi);\\ \theta_g^+ &= C_1^+ a_{11} exp(\lambda_1 \xi) + C_2^+ a_{21};\\ \theta_s^+ &= C_1^+ a_{13} exp(\lambda_1 \xi) + C_2^+ a_{23}.\end{aligned} \tag{63}$$

The condition

$$C_2^+ = 0, \tag{64}$$

is necessary so that Eq. (63) can be used correctly for the products, because

$$\left.\frac{d\theta_s^+}{d\xi}\right|_{\xi\to\infty} = \lim_{\xi\to\infty}(C_1^+ a_{13}\lambda_1 exp(\lambda_1\xi) + C_2^+ a_{23}\lambda_2) = 0.$$

As a result, in this case, it is obtained that:

$$\begin{aligned}&\lambda_1 \approx \frac{1}{2}\frac{K_c}{K_\lambda}\left[1-\sqrt{1+4\alpha\left(\frac{K_\lambda}{K_c}\right)^2}\right] < 0; \quad \lambda_2 \approx -\frac{A}{\varepsilon(1+\bar{u})} < 0;\\ &\lambda_3 \approx \frac{1}{2}\frac{K_c}{K_\lambda}\left[1+\sqrt{1+4\alpha\left(\frac{K_\lambda}{K_c}\right)^2}\right] > 0; \quad \lambda_4 \approx 1+\bar{u} \approx \bar{u} > 0.\end{aligned} \tag{65}$$

Now, it can be depict the stationary solution for the described cases.

4. Algorithm for the stationary solution

Using the parameters presented in [12,22,23]

$$\varepsilon = 0.4, \quad \rho_g = 1.13, \quad \rho_s = 3987\ \text{kg/m}^3, \quad \lambda_g = 0.073,$$
$$\lambda_s = 6\ \text{W/(m K)}, \quad c_g = 1160, \quad c_s = 1300\ \text{J/(kg K)},$$

we get

$$t_* = \frac{\lambda_g}{V_n^2 c_g \rho_g} \approx 10^{-3} \div 10^{-2}\ \text{s}; \quad A = \frac{\alpha t_*}{c_g\rho_g} \approx 1.56 \div 0.027;$$
$$K_\lambda \approx 82.2, \quad \varepsilon(1-\varepsilon)K_\lambda \approx 19.73.$$

Therefore, in this case, when $K_c/K_\lambda \approx 50$, the condition $\frac{A^2}{\varepsilon(1-\varepsilon)K_\lambda} << 1$ is a very good approximation for a qualitative analysis of the problem.

The calculation algorithm is the following: using the values of parameters A, K_c, K_λ, ε, are calculated the roots of the characteristic equation in the way:

$$\begin{aligned}&\lambda_1 \approx \frac{1}{2}\frac{K_c}{K_\lambda}\left[1-\sqrt{1+4\alpha\left(\frac{K_\lambda}{K_c}\right)^2}\right]; \quad \lambda_2 \approx -\frac{A}{\varepsilon(1+\bar{u})};\\ &\lambda_3 \approx \frac{1}{2}\frac{K_c}{K_\lambda}\left[1+\sqrt{1+4\alpha\left(\frac{K_\lambda}{K_c}\right)^2}\right]; \quad \lambda_4 \approx 1+\bar{u} \approx \bar{u},\end{aligned}$$

where

$$\alpha = \frac{BK_c}{(1-\varepsilon)K_\lambda} + \frac{A}{(1-\varepsilon)K_\lambda}. \tag{66}$$

The eigenvalues calculated for some values of the parameters are presented in Table 1.

Now, using λ_i we can calculate the components of vectors $\mathbf{a}_i$ from Eq. (53) and the integration constants with the help of Eq. (58). Expressions (54) allow the calculation of the temperature for the solid phase and for the gas in the reactant region and in the products region.

5. Analysis and discussion

The fuel mass fraction value before and after the reaction front can be found from

$$\eta^- = 1 - \frac{1}{1+\bar{u}} exp\left(\frac{1+\bar{u}}{Le}\xi\right); \quad \eta^+ = \frac{\bar{u}}{1+\bar{u}}. \tag{67}$$

According to these results it can be seen that the Lewis number has no influence on the characteristics of the temperature field.

The mathematical model developed has been based on a flame sheet approximation for the reaction zone, in which the combustion front is treated as a delta function-like region for the reaction. In this way the model provides a discontinuous jump in the gas temperature that can be significantly different from the solid temperature. The replacement of the reaction term by an energy release, of the Dirac delta type function [14,27], eliminates the need for the use of an expression for the combustion rate. From the physical point of view, the physical domain can be divided into a pre-reaction and a post-reaction zone.

The slow speed of the combustion wave and the radiative heat transfer which occurs in the solid tends to equilibrate major tem-

Table 1
Values of the parameter set for the mathematical model solution.

Variant	A	B	$\bar{u}$	λ_1	λ_2	λ_3	λ_4
1	0.75	0.1	100	−1.664e-1	−1.86e-2	50.166	101
2	0.5	0.1	100	−1.663e-1	−1.237e-2	50.166	101
3	0.25	0.1	100	−1.662e-1	−6.188e-3	50.166	101
4	0.15	0.1	100	−1.661e-1	−3.713e-3	50.166	101
5	0.75	0.5	100	−8.202e-1	−1.856e-2	50.82	101
6	0.75	0.3	100	−4.954e-1	−1.856e-2	50.495	101
7	0.75	0.1	−100	−99	−1.664e-1	1.894e-2	50.166
8	0.75	0.1	−80	−79	−1.664e-1	2.374e-2	50.166
9	0.75	0.1	−50	−49	−1.664e-1	3.8265e-2	50.166
10	0.9	0.1	−50	−49	−1.664e-1	4.592e-2	50.166

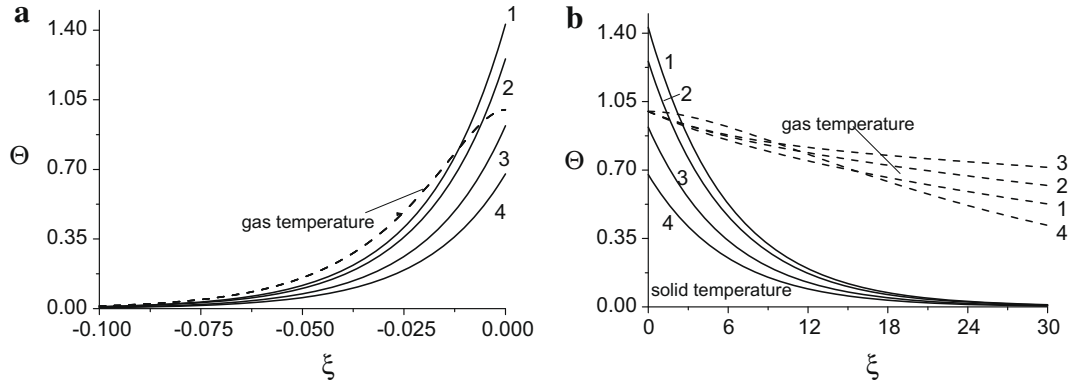

Fig. 2. Temperature distributions. (a) In the reactants region ($\xi < 0$) and (b) behind the reaction front ($\xi > 0$). $\bar{u} = 100$, $B = 0.1$. 1 – $A = 0.75$; 2 – $A = 0.5$; 3 – $A = 0.25$; 4 –$A = 0.15$.

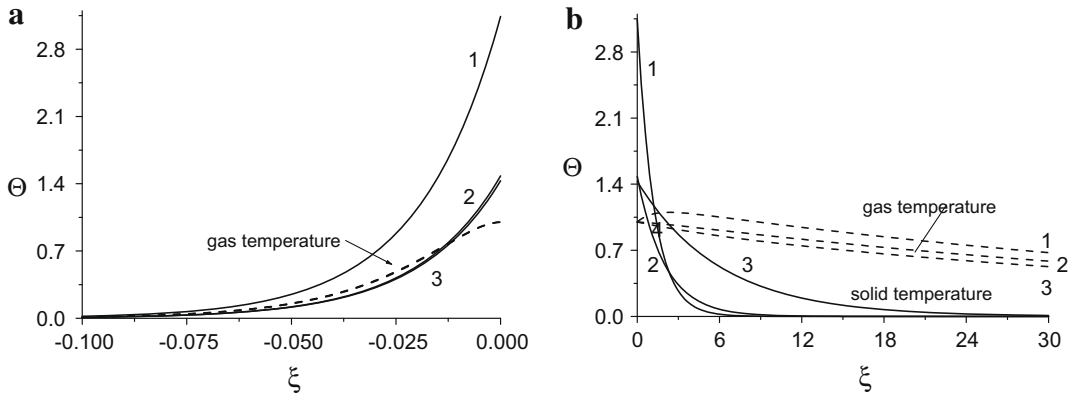

Fig. 3. Temperature distributions. (a) In the reactants region ($\xi < 0$) and (b) behind the reaction front ($\xi > 0$). $\bar{u} = 100$, $A = 0.75$. 1 – $B = 0.5$; 2 – $B = 0.3$; 3 – $B = 0.1$.

perature differences. Even though the objective of this paper has not been to study the effect of radiation, the model developed allows: (a) an implicit interpretation of the role of radiation by redefining the total heat transfer coefficient by two terms: a convective and a radiative component, and (b) by changing the value of the solid to gas thermal conductivity ratio, parameter K_λ in Eq. (21), in which λ_s is defined as the porous medium effective thermal conductivity, that includes the influence of radiation, assuming an optically thick region around the high-temperature zone in the bed [12,14].

The stationary solution is graphically presented in Figs. 2 and 3. Because the spatial scales before and after the reaction front, located at $\xi = 0$, are very different, it is convenient to present the temperature distribution before and after the reaction front in different pictures, (a) and (b). The dotted lines in these figures correspond to the gas temperature and the continuous lines correspond to the solid matrix temperature.

When $\bar{u} > 0$, the spatial scale in the reactants is lower than in the products. For this case, the temperature distribution is presented in Fig. 2. Naturally, the gas temperature in the front is equal to unity. As can be seen from the figures, for different values of A analyzed in Table 1 the temperature of the gas and solid in the front can be very different from each other, depending on the gas and solid thermal–physical properties, which define heat conduction in the system, and on the convective heat transfer in the gas phase.

Fig. 3 illustrates the influence of heat losses, which are defined by coefficient B, to the environment on the front structure. As expected, increasing heat loss to the surroundings leads to a decrease in the maximum temperature of the solid over the investigated range of coefficient B, while the gas temperature changes very little. The calculations show that in the case when $\bar{u} < 0$, the solid matrix is not warmed up.

6. Conclusions

A theoretical analysis of low-velocity filtration combustion based on a two-temperature formulation has been presented. The reaction front is assumed to be small compared to that of the preheat zone. As a result, a stationary analytical solution that considers the difference in physical properties of solid and gas, and heat transport by convection and conduction in the gas phase has been obtained for the first time.

The qualitative difference in the combustion front structure in the cases when it moves downstream and upstream was demonstrated. A variation of the Lewis number magnitude (when it is different from one) was found that does not affect the characteristics of the temperature field in the stationary wave. However, we believe that when the Lewis number is different from one, stability of a combustion wave can become an interesting and important property, which may lead to further investigations.

Acknowledgements

The authors acknowledge the support of CONICYT-Chile under FONDECYT Projects 1040148 and 7040130, and Academia Politécnica Aeronáutica of FACH-Chile.

References

[1] M.S. Mössbauer, O. Pickenäcker, K. Pickenäcker, D. Trimis, Application of the porous burner technology in energy and heat-engineering, in: Fifth International Conference on Technologies and Combustion for a Clean Environment (Clean Air V), Lisbon, Portugal, 1999, pp. 519–523.

[2] J.R. Howell, M.J. Hall, J.L. Ellzey, Combustion of hydrocarbon fuels within porous inert media, Prog. Energy Combust. Sci. 22 (2) (1996) 122–145.

[3] D. Trimis, F. Durst, Combustion in a porous medium – advances and applications, Combust. Sci. Technol. 121 (1997) 153–168.

[4] J.P. Bingue, A.V. Saveliev, A.A. Fridmann, L.A. Kennedy, Hydrogen production in ultra-rich filtration combustion of methane and hydrogen sulphide, Int. J. Hydr. Energy 27 (2002) 643–649.

[5] A.P. Aldushin, I.E. Rumanov, J.B. Matkowsky, Maximal energy accumulation in a superadiabatic filtration combustion wave, Combust. Flame 118 (1999) 76–90.

[6] A.M. Oliveira, M. Kaviany, Nonequilibrium in the transport of heat and reactants in combustion in porous media, Prog. Energy Combust. Sci. 27 (2001) 523–545.

[7] V.S. Babkin, Filtration combustion of gases. Present state of affairs and prospects, Pure Appl. Chem. 65 (2) (1993) 335–344.

[8] S.B. Sathe, R.E. Peck, T.W. Tong, A numerical analysis of heat transfer and combustion in porous radiant burners, Int. J. Heat Mass Transfer 33 (6) (1990) 1331–1338.

[9] J.G. Hoffmann, R. Echigo, H. Yoshida, S. Tada, Experimental study on combustion in porous media with a reciprocating flow system, Combust. Flame 111 (1997) 32–46.

[10] P.H. Bouma, L.P.H. Goey, Premixed combustion on ceramic foam burners, Combust. Flame 119 (1999) 133–143.

[11] M.R. Henneke, J.L. Ellzey, Modelling of filtration combustion in a packed bed, Combust. Flame 117 (1999) 832–840.

[12] S.I. Foutko, S.I. Shabunya, S.A. Zhdanok, Superadiabatic combustion wave in a diluted methane–air mixture under filtration in a packed bed, in: 26th International Symposium on Combustion, The Combustion Institute, Minsk, Belarus, 1996.

[13] K.V. Dobrego, I.M. Kozlov, V.I. Bubnovich, C.E. Rosas, Dynamics of filtration combustion front perturbation in the tubular porous media burner, Int. J. Heat Mass Transfer 46 (2003) 3279–3289.

[14] S.A. Zhdanok, L.A. Kennedy, G. Koester, Superadiabatic combustion of methane–air mixtures under filtration in a packed bed, Combust. Flame 100 (1–2) (1995) 221–231.

[15] W.M. Mathis Jr., J.L. Ellzey, Flame stabilization, operating range, and emissions for methane/air porous burner, Combust. Sci. Technol. 175 (2003) 825–839.

[16] Y. Xuan, R. Viskanta, Numerical investigation of a porous matrix combustor-heater, Numer. Heat Transfer Part A 36 (1999) 359–374.

[17] I.Y. Akkutlu, Y.C. Yortsos, The dynamics of in-situ combustion fronts in porous media, Combust. Flame 134 (2003) 229–247.

[18] L.A. Kennedy, J.P. Bingue, A. Saveliev, A.A. Fridmann, S.I. Foutko, Chemical structures of methane–air filtration combustion waves for fuel-lean and fuel-rich conditions, Proc. Combust. Inst. 28 (2000) 1431–1438.

[19] K.G. Shkadinsky, G.V. Shkadinskaya, B.J. Matkowsky, Filtration combustion in moving media: one and two reaction zone structures, Combust. Flame 110 (1997) 441–461.

[20] S.R. Turns, An Introduction to Combustion: Concepts and Applications, second ed., McGraw Hill, New York, 1996. pp. 472-507.

[21] G. Brenner, K. Pickenäcker, O. Pickenäcker, D. Trimis, K. Wawrzinek, T. Weber, Numerical and experimental investigation of matrix-stabilized methane/air combustion in porous inert media, Combust. Flame 123 (2000) 201–213.

[22] I.Y. Akkutlu, Y.C. Yortsos, The effect of heterogeneity on in-situ combustion: propagation of combustion fronts in layered porous media, SPE J. 10 (4) (2005) 394–404.

[23] V.I. Bubnovich, S.A. Zhdanok, K.V. Dobrego, Analytical study of combustion waves propagation under filtration of methane–air mixture in a packed bed, Int. J. Heat Mass Transfer 49 (2006) 2578–2586.

[24] V. Bubnovich, M. Toledo, Analytical modelling of filtration combustion in inert porous media, Appl. Therm. Eng. 27 (7) (2007) 1144–1149.

[25] J.-R. Shi, M.-Zh. Xie, H. Liu, G. Li, L. Zhou, Numerical simulation and theoretical analysis of premixed low-velocity filtration combustion, Int. J. Heat Mass Transfer 51 (7–8) (2008) 1818–1829.

[26] D.A. Frank, Kamenetzki, Diffusia i Teploperedacha v Chimicheskoy Kinetike, Nauka, Moscow, 1987. pp. 346.

[27] V.S. Babkin, Y.M. Laevskii, in: Y.S. Matros (Ed.), Propagation of Heat Waves in Heterogeneous Media, Nauka, Novosibirsk, 1988, p. 108.

[28] A.A. Korzhavin, V.A. Bunev, V.S. Babkin, A.S. Klimenko, Selective diffusion during flame propagation and quenching in a porous medium, Combust. Explosion Shock Waves 41 (4) (2005) 405–413.